Nonlinear input-output models of the radiation belt electron flux driven by geoeffective variables

M. Taylor[1*], I.A. Daglis[1], A. Anastasiadis[1], D. Vassiliadis[2], P. Perakakis[3] and L. Vlahos[4]

[1]Institute for Space Applications and Remote Sensing(ISARS), National Observatory of Athens(NOA), Metaxa and Vasillis Pavlou Street, Penteli, Athens 15236, Greece.
[2]Department of Physics, Hodges Hall, PO Box 6315, West Virginia University, Morgantown, WV 26506-6315, USA.
[3]Department of Pschology, University of Granada, Campus de la Cartuja, Granada 18071, Spain.
[4]Section of Astrophysics, Astronomy and Mechanics, Department of Physics, Aristotle University of Thessaloniki (AUTH), 54006 Thessaloniki, Greece.
email*: michael@space.noa.gr

Introduction

Due to rapid technological progress, state of the art databases now sample the near-Earth space environment over a vast range of spatio-temporal scales from the Earth's surface all the way up to the heliosphere, and from one minute to 24 hour intervals. Time series data exists for a plethora of some 47 parameters relating to space weather [2] and we have collected daily averages between 1993 and 2001 for 11 variables in order to study nonlinear input-output models of the radiation belt energetic electron flux.

Theory

Our modelling approach (see Fig. 1) involves four key steps:

1. Constraining physical models with dimensional analysis
2. Constructing a taxonomy of nonlinear input-output models
3. Representing nonlinear dynamics with FIR neural networks
4. Identification of the physical model

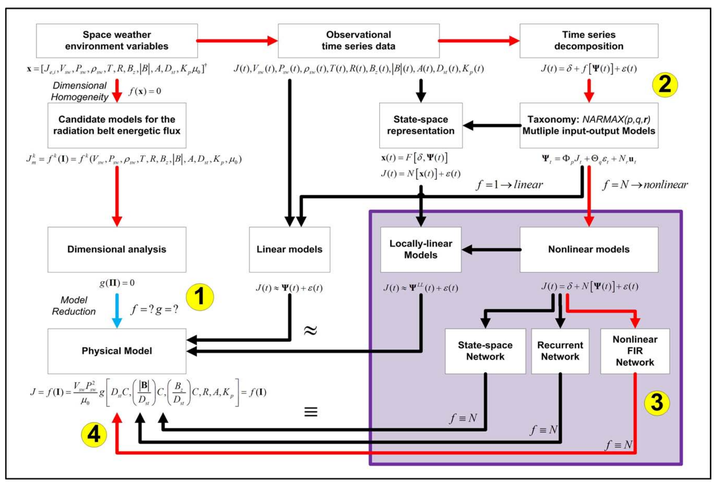

FIG. 1. Our approach is indicated by red arrows. Black arrows relate to other approaches used in the literature. The purple box shows nonlinear models while the blue arrow is indeterminable step.

STEP 1: Constraining physical models with dimensional analysis

We take as our premise the notion that the physics of a space weather environment like the radiation belts is encoded in data measurements of that region such that inter-dependencies between parameters are implicit. The task then, is to decypher and decode these empirical relations in order to make the inter-dependencies explicit. We take as our set $\mathbf{x}$ of relevant physical parameters,

$$\mathbf{x} = (J_{(e,i)}, V_{sw}, P_{sw}, \rho_{sw}, T, R, Bz, |B|, A, Dst, Kp, \mu_0)^{\dagger}. \quad (1)$$

$J_{(e,i)}[MeVcm^{-2}s^{-1}sr^{-1}]$ is the radiation belt energetic flux of electrons or ions, $V_{sw}[kms^{-1}]$, $\rho_{sw}[kgcm^{-3}]$, $P_{sw}[kgcm^{-1}s^{-2}]$ are the solar wind velocity, density and ram pressure, $T[K]$ is the plasma temperature, R is the sunspot number, $Bz[nT]$ and $|\mathbf{B}|[nT]$ are the IMF variables, A is the alpha particle to proton ratio, $D_{st}[nT]$ and K_p are the geomagnetic ring current and planetary indices, and $\mu[Hm^{-1}]$ is the permeability of free space.

One can then construct k-different parameter inter-dependency relation permutations for the electron flux J as the target (output) variable as a function of input drivers $\mathbf{I}$,

$$J^{(k)} = f^{(k)}\Big[V_{sw}, P_{sw}, \rho_{sw}, T, R, B_z, |B|, A, Dst, Kp, \mu_0\Big]. \quad (2)$$

Dimensional homogeneity requires that $f(x_n) = 0$ and, from Buckingham's Theorem, this implies that for r independent parameter dimensions (in this case $r = \{M, L, T, Q\}$), there will be $m = n-r$ dimensionless groups of parameters π_m such that, $g(\pi_m) = 0$. Applying the dimensional analysis similarity transforms [5] to $\mathbf{x}$ then we obtain the relation [6],

$$J = \frac{V_{sw}P_{sw}^2}{\mu_0} g\Big[D_{st}C, |B|\,C, B_zC, R, A, K_p\Big] = f\Big[\mathbf{I}\Big] \quad (3)$$

with $C = (\mu_0\rho_{sw}V_{sw}/P_{sw}^3)^{-1/5}$. We see that, although the function g (and hence f) is yet to be determined, variables are now grouped and we shall see that this helps model identification. Since we work with time series data for each variable, our task is to construct and test nonlinear input-output models of the form $J(t) = f\Big[\mathbf{I}(t)\Big]$ in an attempt to identify f.

STEP 2: Constructing a taxonomy of nonlinear input-output models

We began with a generalisation of the Wold time series decomposition [10] having the form,

$$J_t = \delta + f(\mathbf{\Psi}_t) + \varepsilon_t \equiv \hat{J}_t + \varepsilon_t \quad (4)$$

where J_t is the electron flux time series, $\hat{J}_t = \delta + f(\mathbf{\Psi}_t)$ are the model predictions, f is a general function (linear or nonlinear), δ is a constant (zero in the absence of trend), $\varepsilon_t = J_t - \hat{J}_t$ are the prediction errors and $\mathbf{\Psi}_t$ is an "information matrix" constructed from lag polynomials Φ_p, Θ_q, N_r, lag operators L^i, L^j, L^k and differencing indices d_1, d_2 and which has the general form [6],

$$\mathbf{\Psi}_t = \Phi_p(1-L^i)^{d_1}J_t + \Theta_q\varepsilon_t + N_r(1-L^k)^{d_2}I_t, \quad (5)$$

corresponding to a Nonlinear AutoRegressive Integrated Moving-Average eXogenous input NARIMAX(p, d_1, q, d_2, r) process. Note that in the case of multiple inputs, I_t will be a vector $\mathbf{I}_t$. The information matrix then contains operators acting on time-delayed (lagged) time series of electron flux J_{t-p} (autoregression AR), lagged equation errors ε_{t-q} (moving-average MA), and lagged inputs I_{t-r} (eXogenous). The particular class of model chosen depends on how exactly $\mathbf{\Psi}_t$ is defined and on the functional form of f. For example, the nonlinear autoregressive, moving-average, exogenous input NARMAX(p, q, r) process has $\mathbf{\Psi}_t = \Phi_pJ_t + \Theta_q\varepsilon_t + N_rI_t$ and represents the time series decomposition,

$$J_t = \delta + f\Big[\ \varphi_1\ J_{t-1}, \cdots, \varphi_pJ_{t-p}, \phi_1\varepsilon_{t-1}, \cdots, \phi_q\varepsilon_{t-q}, \quad (6)$$

$$\eta_1\ I_{t-1}, \cdots, \eta_rI_{t-r}\Big] + \varepsilon_t. \quad (7)$$

The table below shows the complete taxonomy of input-output models we have identified with this class. Armed with input-output relations, we now construct neural networks to model f.

Function	Autoregression order	Moving-Average order	Inputs	Model
1	1	0	0	AR(1)=Random walk
1	p	0	0	AR(p)
1	p	0	r	ARX(p, r)
1	0	q	0	MA(q)
1	0	∞	0	MA(∞)=Wold Decomposition
1	0	q	r	MAX(q, r)
1	p	q	0	ARMA(p, q)
1	p	q	r	ARMAX(p, q, r)
f	p	0	0	NAR(p)
f	p	0	r	NARX(p, r)
f	0	q	0	NMA(q)
f	0	q	r	NMAX(q, r)
f	p	q	0	NARMA(p, q)
f	p	q	r	NARMAX(p, q, r)

STEP 3: Representing nonlinear dynamics with FIR neural networks

The reason we chose networks over other methods [8] is twofold:

1. Takens' Theorem [4] implies a 1-to-1 mapping between a time series and the underlying state space
2. Multi-Layer Perceptrons (MLP) are universal (exact, nonlinear) function approximators [1]

Feedforward MLPs that have lagged inputs create short-term memory and incorporate nonlinear dynamics into the network state space. In the case that neural activation functions are linear then they operate as finite impulse-response (FIR) networks [9]. Linear FIR models already exist in the literature [7]. Here we develop nonlinear (sigmoidal activation function) FIR networks (NFIRs) whose architecture is shown in Figure 2. Referring to the taxonomy we see for example that a single input NFIR network with r-delays models is an NMAX$(0, r)$ process. Additionally, in the case that the outputs $J(t)$ are passed through a delay line of order p and fed in as a network input, then we have a recurrent NFIR network that models the NARMAX$(p, 0, r)$ process.

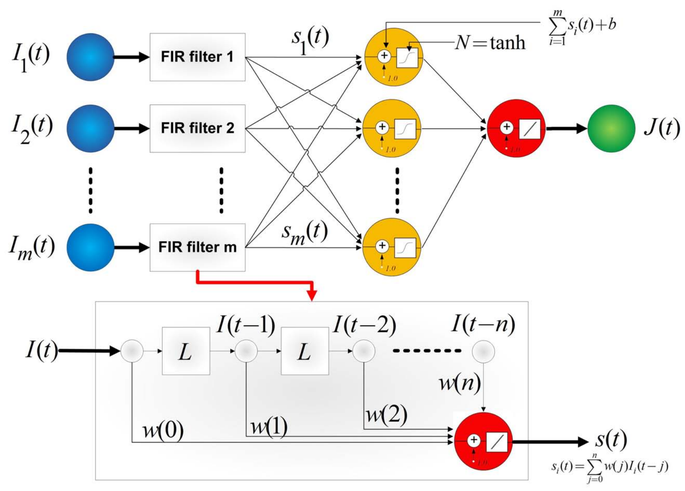

FIG. 2. A schematic diagram of the nonlinear (dynamical) FIR network used in this work.

In order to measure the degree of success in reproducing observed values $J(t)$ from the network model $\hat{J}(t)$, we used the data-model correlation coefficient C:

$$C = \frac{1}{T}\frac{1}{\sigma_J\sigma_{\hat{J}}}\int_0^T \Big(\hat{J}(t) - \Big\langle\hat{J}(t)\Big\rangle\Big)\Big(J(t) - \langle J(t)\rangle\Big)dt \quad (8)$$

where $\langle J(t)\rangle$ and σ_J are the mean and standard deviation of $J(t)$.

STEP 4: Identification of the physical model

Since the neuron activation function and weights (connections) are explicit, the network architecture can be converted into equations with known AR and MA coefficients. We plan to do this next.

Results & Discussion

All network models were trained with the Levenberg-Marquardt backpropagation algorithm [3] for 100 epochs on the complete dataset of daily averages. Figure 3 presents $J(t)$ from 01/01/1993 to 31/12/2001 between $1.1Re \leq L \leq 10.0Re$ binned in intervals of $L = 0.1 = Re/10$. The first zero of autocorrelation function (ACF) implies the lag order. The network models all have 20 delays. In Figure 4, we compare the autoregressive linear FIR model AR(20) [7] with its nonlinear FIR network counterpart NAR(20). The nonlinear network, although more accurate than the linear model is noisier. This is due to the presence of non-zero prediction errors ε_t. Figure 5 shows the results of NMAX$(0, 20)$ predictions for the first 1000 days of the dataset at $L = 5.2$. In these runs, 50 hidden neurons were needed to cope with network learning of the MA process. It is clear that dimensionless variables (Fig.5b and Fig.5c) improve performance.

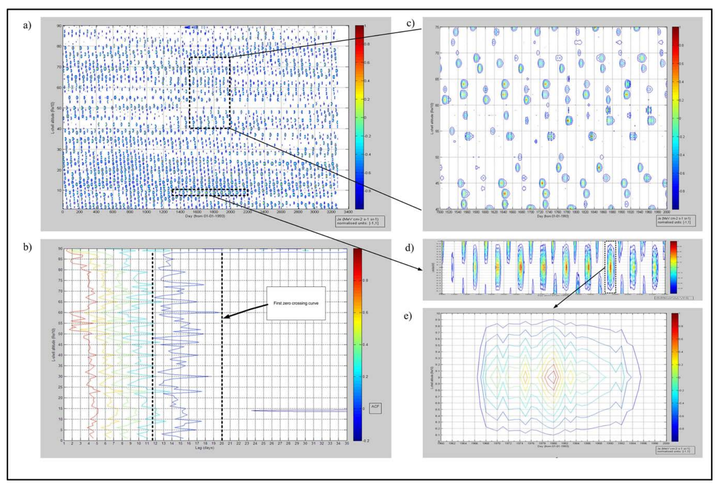

FIG. 3. Normalised values of $J(t)$[-1,1] for: a) the entire dataset, b) the autocorrelation by L-interval, c) the outer-radiation belt region $4.0 \leq L \leq 7.5$, d) suspected temporal evolution of a flux bubble located at $L = 2.0$ and e) the spatio-temporal structure of thw bubble centered at $L = 2.0$ and day 1980.

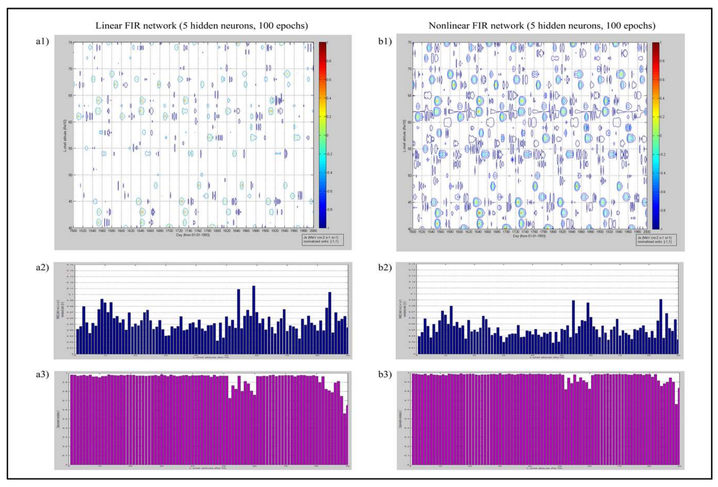

FIG. 4. Autoregressive linear FIR (a) and nonlinear FIR network model (b) of $J()$: a1) and b1) model the outer-radiation belt region $4.0 \leq L \leq 7.5$ spanning the active period instigated at $L = 10.0$ at day 1500 (compare with Fig.3c), a2) and b2) present the root mean-square errors $RMSE \equiv \sqrt{\sum(\varepsilon_t)}$, and a3) and b3) are the representative data-model correlations.

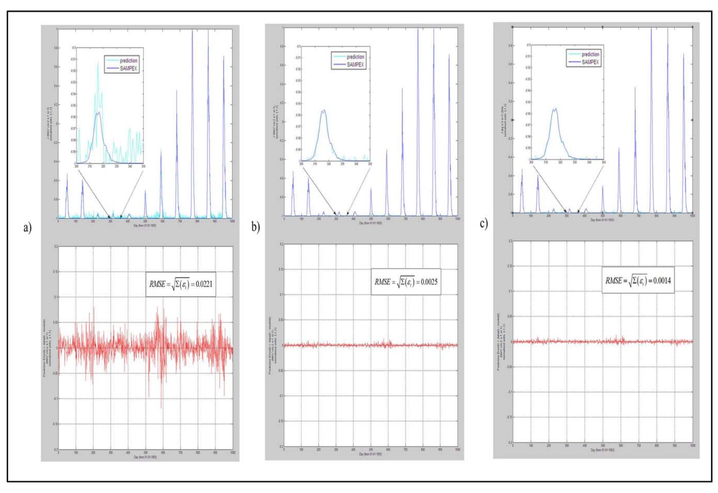

FIG. 5. Nonlinear moving-average FIR network prediction NMAX$(0, 20)$ for the first 1000 days at $L = 5.2$: a) $I(t) = D_{st}$, b) $I(t) = K_p$ and c) $I(t) = D_{st}C$. Upper panels show the data and model predictions. Lower panels show prediction errors $\varepsilon(t)$.

Acknowledgements

MT thanks ISARS-NOA for their hospitality and support and the Greek State Scholarship Foundation (IKY) for financial support.

References

[1] Hornik J, Stinchombe M, White H (1989) Mutlilayer feedforward networks are universal approximators. *Neural Networks* 2:359-366.

[2] OMNI (2009) OMNIweb data explorer. *http://omniweb.gsfc.nasa.gov/form/dx1.html.*

[3] Rumelhart D-E, McClelland J-L (1986) Parallel distributed processing: explorations in the microstructure of cognition. *MIT Press* (Cambridge, MA).

[4] Takens P (1981) Detecting strange attractors in fluid turbulence, In: Rand D and Young L-S (1981) Dynamical Systems and Turbulence. *Springer* (Berlin) 898:366-381.

[5] Taylor M, Diaz A-I, Jodar-Sanchez L-A, Villanueva-Mico R-J (2008) A matrix generalisation of dimensional analysis: new similarity transforms to address the problem of uniqueness. *Adv Studies Theor Phys* 2(20):979-995.

[6] Taylor M, Daglis I-A, Anastasiadis A, Vassiliadis D, Vlahos L (2009) A taxonomy of input-output models for the radiation belt enegetic electron flux driven by geoeffective parameters. (in preparation).

[7] Vassiliadis D, Fung SF, Klimas AJ (2005) Solar, interplanetary and magnetospheric parameters for the radiation belt energetic electron flux. *J Geophys Res* 110:1-12.

[8] Vassiliadis D (2007) Forecasting space weather, In: Bothmer V, Daglis I-A (eds) (2007) Space weather: physics and effects. *Springer-Praxis* (Berlin).

[9] Wan E-A (1993) FIR neural networks for autoregressive time series prediction, In: Weigand A, Gershenfeld N (eds) (1993) Proceedings of the NATO advanced workshop on time series prediction and analysis (Santa Fe, NM). *Addison-Wesley.*

[10] Wold H (1954) A Study in the Analysis of Stationary Time Series. *Almqvist and Wiksell* (Uppsala).